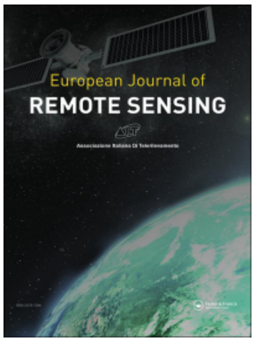

European Journal of Remote Sensing

ISSN: (Print) (Online) Journal homepage: https://www.tandfonline.com/loi/tejr20

Integrating Copernicus land cover data into the i-Tree Cool Air model to evaluate and map urban heat mitigation by tree cover

Rocco Pace, Francesca Chiocchini, Maurizio Sarti, Theodore A. Endreny, Carlo Calfapietra & Marco Ciolfi

EUROPEAN JOURNAL OF REMOTE SENSING
https://doi.org/10.1080/22797254.2022.2125833

Taylor & Francis
Taylor & Francis Group

RESEARCH ARTICLE

OPEN ACCESS Check for updates

Integrating Copernicus land cover data into the i-Tree Cool Air model to evaluate and map urban heat mitigation by tree cover

Rocco Pace[a,b], Francesca Chiocchini[a], Maurizio Sarti[a], Theodore A. Endreny[c], Carlo Calfapietra[a] and Marco Ciolfi[a]

[a]Research Institute on Terrestrial Ecosystems (IRET), National Research Council (CNR), Porano, Italy; [b]Institute of Meteorology and Climate Research, Atmospheric Environmental Research (IMK-IFU), Karlsruhe Institute of Technology (KIT), Garmisch-Partenkirchen, Germany; [c]Department of Environmental Resources Engineering, SUNY ESF, Syracuse, NY, USA

ABSTRACT
Cities host more than half of the world's population and due to global warming and land use change their vulnerability to deadly heat waves has increased. A healthy vegetated landscape can abate heat wave severity and diminish the related urban heat island through the process of evapotranspiration. This research aimed to develop a methodology for cities to use publicly available Copernicus land cover maps within the i-Tree Cool Air water and energy balance model to map air temperature and humidity. The manuscript presents proof of concept using Naples, Italy with its Mediterranean climate characterized by limited soil water for cooling via evapotranspiration. The approach achieved strong correlations between predicted and observed air temperatures across the city ($r \geq 0.89$). During the warm season of 2020, forested land cover was 5°C cooler than land cover dominated by impervious cover. Simulated land cover change, limited to a 10% increase or decrease in tree cover, generated an inverse change of 0.2°C in maximum hourly air temperature, with more trees obtaining cooler air. Soil water limited the cooling, with the generally wetter spring season enabling greater cooling of air temperatures, and summer droughts without irrigation had constrained cooling. Sustainable urban design will likely require an increase in plant cover along with a reduction of impervious surfaces that absorb and reradiate heat in order to improve community resilience to heat waves.

ARTICLE HISTORY
Received 18 March 2022
Revised 11 July 2022
Accepted 13 September 2022

KEYWORDS
Heat waves; urban trees; temperature reduction; mediterranean city; Urban Atlas; ecosystem services

Introduction

A threatening consequence of global warming is the increased frequency and intensity of heat waves (Meehl & Tebaldi, 2004; Russo et al., 2014). The health risks associated with the intensification of heat waves are considerable (Baldwin et al., 2019), especially for the vulnerable population (McGeehin & Mirabelli, 2001). A single heat wave during the summer of 2003 caused 70,000 deaths in Europe (Robine et al., 2008), and a heat wave during July 2010 in Moscow caused approximately 56,000 deaths (Rahmstorf & Coumou, 2011). The intensification of heat waves has been attributed to climate change, which exacerbates the effect of land cover change and growth of urban populations, leading to hotter summers in urban areas (Guerreiro et al., 2018). Prior to climate change urban areas were hotter than rural areas due to the diminished vegetation cover, heat absorbing structures, and concentrated anthropogenic heat production, e.g. warming homes, powering industry. This phenomenon of hot urban areas surrounded by cooler rural areas is called the urban heat island (UHI), and the UHI makes urban areas more susceptible to heat waves (D. Li & Bou-Zeid, 2013; Ward et al., 2016). As a result, heat waves in urban areas are likely to be more severe than in rural areas due to the additive effects of UHI-related warming (Founda et al., 2015; He et al., 2021; Rizvi et al., 2019), which vary according to land use characteristics and weather conditions, with generally more intense effects in areas characterized by densely built structures and low wind speed conditions (Ngarambe et al., 2020).

Efforts to cool cities with air conditioning powered by fossil fuels will intensify the problem, releasing additional anthropogenic heat and greenhouse gases. Urban areas currently generate approximately 70% of the anthropogenic greenhouse gas emissions (UN-Habitat, 2020), which cause heat wave intensification (Guo et al., 2018). Urban planning demands effective climate change adaptation and mitigation strategies by cities to minimize the impacts of heat waves (Haines et al., 2006). The pursuit of urban greening strategies, often employed for stormwater management such as nature-based solutions, can theoretically contribute to adaptation, e.g. cooling the air, and mitigation, e.g. sequestering carbon (Norton et al., 2015; WWAP, 2018). Indeed, the use of effective green infrastructure can offset the UHI impact during heat waves, which

CONTACT Francesca Chiocchini francesca.chiocchini@cnr.it Research Institute on Terrestrial Ecosystems (IRET), National Research Council (CNR), Porano, TR, Italy
Supplemental data for this article can be accessed online at https://doi.org/10.1080/22797254.2022.2125833

are increasingly frequent and intense in a future warmer climate (Tewari et al., 2019).

Field studies have documented the cooling impact of evapotranspiration during summer days, often using sampling transects that pass from vegetated to impervious cover, with vegetated areas ranging from 1°C to 6°C cooler than areas with impervious cover (Bowler et al., 2010a; Oliveira et al., 2011). Heterogeneity in land cover and use contributes to the limitations (Ziter et al., 2019), and cities have high spatial and temporal heterogeneity in land cover and use classes. While urban impervious spaces often prevail over green ones, imperviousness and trees can co-occur at the same place, e.g. in tree-lined avenues. The interaction between impervious surface cover and tree canopy cover influences air temperature over the urban area, depending on their spatial arrangement, extent, and distribution (Cadenasso et al., 2007). Obtaining a landscape perspective of how urban greening contributes to microclimate regulation is complex and laborious using in-situ observations, while remote sensing aerial or satellite approaches are limited to measuring land surface temperatures, not air temperature (Klok et al., 2012; Sobrino et al., 2012; Zhang et al., 2017). Ambitious studies have deployed vehicles along roadways to obtain tens of thousands of air temperature measurements each hour, and then statistically regressed those air temperature data with their corresponding land cover and use data, derived from remotely sensed satellite imagery (Shandas et al., 2019). The statistical regression between observed air temperature and land cover allowed researchers to extend their estimates of the atmospheric UHI across the entire city, beyond the roads, but the map was only good for that one hour of that day (Shandas et al., 2019). The integration of remotely sensed land cover data with models that estimate how vegetation cover can regulate air temperature is a promising way forward in designing urban resilience (Smith et al., 2021).

There is great utility in making accurate predictions of how urban greening can enable greater evapotranspiration to partition net radiation into cooler air temperatures, allowing the design of more resilient communities. To support such predictions, scientists have developed techniques to better understand how plants transpire water, using tools that measure water release through plant leaf stomata (Konarska et al., 2016) or measure sap flux density through plant stems as transpiration rates (Rahman et al., 2017). In such studies the effect of evapotranspiration on air temperature can be directly measured with thermistors that detect changes in sensible heat, or remotely with indirect radiation detection, such as handheld or satellite infrared cameras using charged coupled devices that receive the land surface skin outgoing longwave radiation and infer the surface temperature (Massetti et al., 2019; Speak et al., 2020). Urban tree canopy temperatures were also measured and vary according to species, land cover type and weather conditions (Meier & Scherer, 2012; Rahman et al., 2017). Unfortunately, these in-situ measurement techniques have fallen short in their ability to characterize air temperature across the urban unit and over extended time periods.

Mechanistic models, defined as representing the biophysical processes involved in evapotranspiration, have the potential to overcome the limitations of measurements and of statistical models constrained to the place and time of their measurements. These mechanistic models can characterize how the distribution of water and land cover interact to regulate the air temperature of cities. While three dimensional computational fluid dynamics models can resolve the interaction of vegetation and turbulent winds on the evolution of microclimate (Buccolieri et al., 2018), these models require detailed computational cells and parameterization that make them infeasible for city scale applications. More feasible are one dimensional mechanistic models using inputs of tree structure and meteorological time series, which have proved accurate in predicting how evapotranspiration regulated air temperature about trees plots within cities (Pace et al., 2021; Rötzer et al., 2019). The detailed tree structure or boundary condition data used by such models has limited them to assessments of heat mitigation by vegetation only at a limited spatial or temporal scale (Gatto et al., 2021; Zölch et al., 2016).

Urban canopy models incorporated tree processes into their energy balance (Krayenhoff et al., 2014; Lee & Park, 2008) and explicitly consider the radiative shading, evapotranspiration, and root water uptake of urban trees in street canyons and evaluate thermal comfort conditions at street level (Redon et al., 2020; Wang et al., 2021). A suitable city-scale and parsimonious approach to model inputs is provided by the one dimensional mechanistic i-Tree Cool Air model, described as a physically based analytical spatial air temperature and humidity model, which simulates the water and energy balance of evapotranspiration (Y. Yang et al., 2013). The i-Tree Cool Air model uses remotely sensed inputs of land cover derived for the US along with time series data from a single weather station to estimate the air temperature across mesoregions, and has evaluated the heat mitigation by urban tree cover and the related health effects for US cities (Sinha et al., 2021, 2022). Authors estimated spatially and temporally explicit reductions in temperature and heat-related mortality associated with a 10% increase in tree cover in several U.S. cities. The reduction of heat-related mortality vary widely across cities, in function of demographics, land cover, and local climatic conditions, with higher percentage in reduction for hotter and drier cities. Model results were compared with urban weather stations in Syracuse, NY, achieving a good correlation for air (R^2 from 0.81 to 0.99) and dewpoint temperature (R^2 from 0.81 to 0.99; Y. Yang et al., 2013). So far, this model was only tested and applied for United States locations, where urban settings, tree/impervious cover and weather conditions can be very different and produce different results.

The aim of this manuscript was to develop a methodology for European cities to use remotely sensed land cover maps within a water and energy balance model that predicts how urban greening mitigates heat waves. The manuscript addresses the following questions: 1) How can heat mitigation by tree cover be assessed for European cities at city scale? 2) How much does tree cover contribute to heat mitigation in a Mediterranean city characterized by a pronounced summer drought? 3) How reliable are the model estimates? 4) How much could an increase or decrease in tree cover affect heat mitigation? and 5) How can these results support urban planning? This study chose to a proof of concept the city of Naples, a metropolitan city in southern Italy characterized by a pronounced Mediterranean climate, which limits water available for evapotranspiration, high rate of urbanization and population density coupled with a low percentage of tree cover and limited in some areas. The study focused on the whole warm season of 2020 (April–October) and the hottest day of the year (August 9), and examined how changes in land cover affect the urban heat. The proposed methodology uses satellite-derived land cover data that is shared across Europe to establish the base-case cover. This approach can be used by any European city to evaluate nature-based heat wave mitigation strategies and inform climate adaptation and mitigation plans.

Materials and methods

Study site

The municipality of Naples is located on the Gulf of Naples on the western coast of southern Italy (Figure 1a), covering an area of 117 km^2 and containing a densely populated core with over 900,000 residents (ISTAT, 2021a), surrounded by a metropolitan population of 3 million. Naples is one of the larger and more densely populated urban areas in the Mediterranean region, which has a signature climate with winter precipitation and extended summer droughts. Between 2010 and 2020 Naples had an average annual temperature of 17.3 °C and annual total precipitation of 753.1 mm (ISTAT, 2021b).

I-Tree Cool Air model and inputs of land cover class

The i-Tree Cool Air model (https://www.itreetools.org/tools/research-suite/hydro-plus) simulates the effect of vegetation on the vertical water and energy balance across space to predict hourly air temperature and humidity for use in sustainable urban planning, such as abating the UHI effect (Y. Yang et al., 2013). For more details on the energy and water balance equations see Y. Yang et al. (2013). The i-Tree Cool Air model was designed to use few and readily available inputs, which include: a) a time series record of meteorological measurements from a single reference weather station; b) raster maps in ASCII format of terrain elevation (m), tree canopy cover (%), impervious surface cover (%), and land cover class; and c) parameter values for terms in the water and energy equations within an XML file (Sinha et al., 2021; Y. Yang et al., 2013). The model uses physically based analytical equations that balance short and longwave radiation with land surface latent and sensible heat emissions, modulated by surface and atmospheric resistances (Y. Yang et al., 2013). In this application, the i-Tree Cool Air model was operated using the default water and energy parameters (Y. Yang et al., 2013).

The model output provides raster maps or time series of estimated temperature and humidity, from hourly or coarser resolutions, and temperatures from groups of map pixels can be averaged using a raster map input of block groups. The model was designed to obtain land cover class from the National Land Cover Database (NLCD) layers, which are derived from National Aeronautics Space Agency (NASA) Landsat satellite imagery at a spatial resolution at 30 m using Anderson level-2 classification, and are provided by the Multi-Resolution Land Cover Consortium (MRLC) (https://www.mrlc.gov/viewer/). These NLCD Anderson level-2 land cover classes are organized so values in the 10s designate water, values in the 20s designate developed, values in the 30s are barren, values in the 40s are forest, etc., through values in the 90s which are wetlands (Figure 1f). These MRLC derived land cover class inputs are available for the United States of America, but not for other parts of the world, and methods follow for using a widely available European land cover dataset within i-Tree Cool Air.

European land cover and elevation data as inputs to i-Tree Cool Air model

The European Copernicus Land Monitoring Service (CLMS) (https://land.copernicus.eu/) data products were processed in this research to comply with i-Tree Cool Air model input requirements. These publicly available CLMS data are based on the European

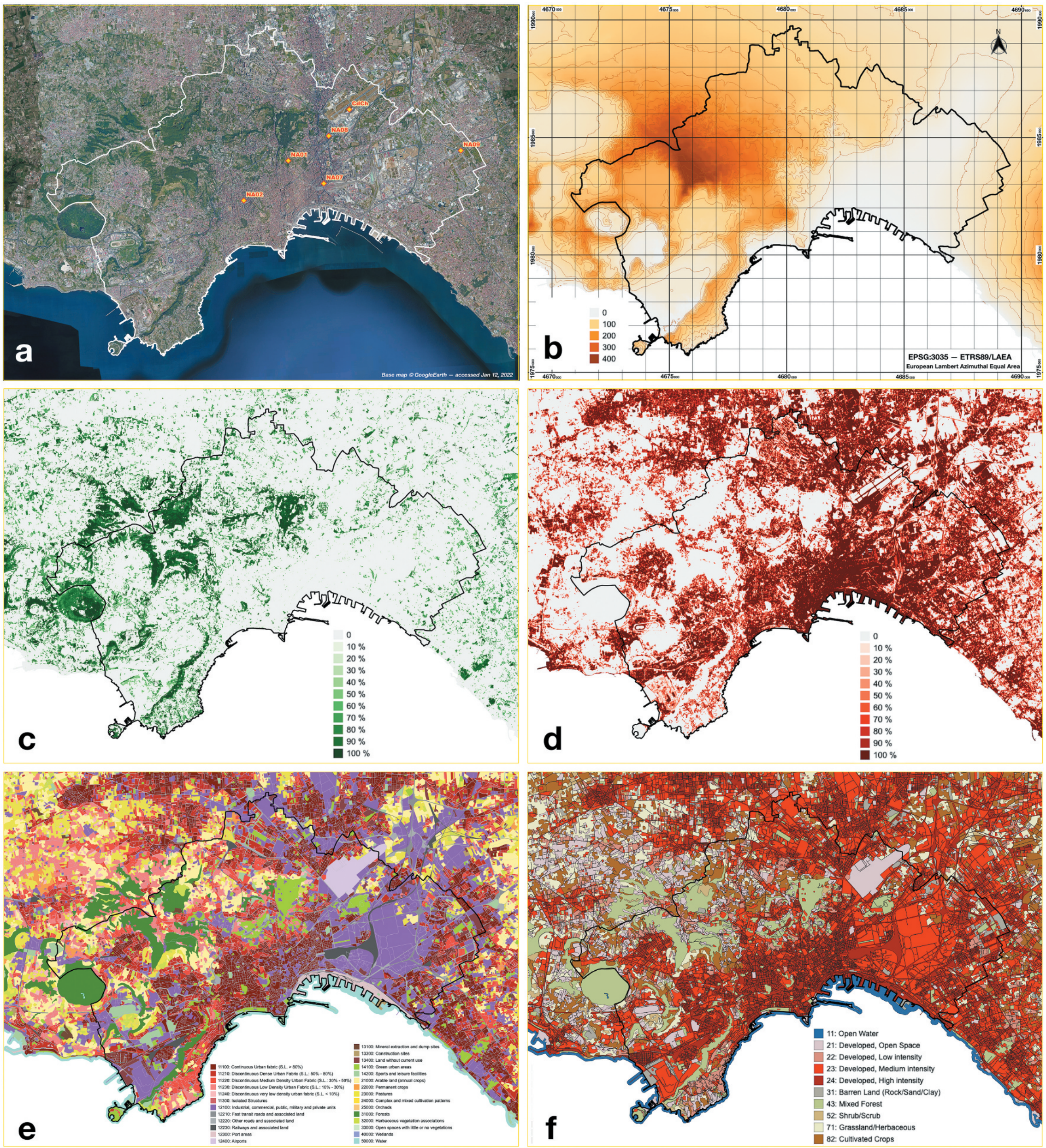

Figure 1. Geographical overview of the study area with weather stations (a) and input spatial data for the model simulation: DEM (b), tree cover density (c), imperviousness density (d), UA land cover from Copernicus (e) and US NLCD (d) (the figure is available full-page in the Supplementary 7).

Space Agency's (ESA) Sentinel-1 and Sentinel-2 satellites imagery and provide land cover, land use and changes, vegetation state, water cycle and earth surface energy variables across the Europe Union. They include the Urban Atlas (UA) at 10 m spatial resolution and part of the High-Resolution Layers (HRL) using Very-High-Resolution (VHR) satellite imagery. In addition to raster data, the UA offers VHR vector-based land cover and land use maps of European major cities, defined as more than 50,000 inhabitants, and their surroundings areas. The delineation of these areas is done in accordance with the Functional Urban Areas classification (FUA), with a minimum mapping unit of 0.25 ha in urban areas and 1 ha in rural ones. These HR and VHR images were classified into land cover through a combination of automatic and interactive rule-based classification for several reference years. In this study, the following CLMS data from the 2018 reference year were resampled at 30 m resolution, according to US equivalent standards: 1) Tree cover density (TCD), a raster dataset, providing information about the level of TCD in a range from 0% to 100% (Figure 1c); 2) Imperviousness Density (IMD), a raster dataset, representing the percentage of land covered by artificial soil sealing, also ranging 0% to 100% (Figure 1d); and 3) UA land use and land cover map, a vector dataset, providing the baseline of land use and land cover based on FUA (Figure 1e).

The European CLMS UA land use/land cover classification (Figure 1e), derived from CORINE land cover, is composed of 27 classes pertaining to five thematic groups: the Artificial Surfaces, or class 1, divided into four hierarchical levels of classification; the Agricultural Areas, or class 2, divided into two hierarchical levels, as well as the Natural and (semi-) natural Areas (class 3), the Wetlands Areas (class 4) and Water Areas (class 5). This contrasts with the default i-Tree Cool Air model Anderson level-2 land cover inputs consisting of nine land cover categories (urban or built-up; agricultural; range; forest; water; wetland; barren; tundra; and perennial snow and ice), and 37 subcategories, representing two hierarchical levels of classification. The CLMS UA map of land use/land cover was reclassified to fit the NLCD Anderson level-2 classes, following a multi-to-one maximum likelihood criterion: we assigned one or more CLMS UA classes to each NLCD class, according to the class taxonomy, using a translation between products reported in Table 1 and performed the reclassification with QGIS vector toolbox.

The raster elevation data for the i-Tree Cool Air model can come from essentially any Digital Elevation Model (DEM) product, including the Shuttle Ranging Topography Mission (SRTM) data which provides global coverage at 90 m resolution; the data simply need to be resampled to match the spatial resolution of the land cover data. In this application, a local Italian DEM dataset product of 20 m resolution (http://www.pcn.minambiente.it/mattm/en/view-service-wms/) was used and resampled to 30 m resolution for spatial congruence with land cover data (Figure 1b). The i-Tree Cool Air model processes these DEM data into aspect and slope for each map pixel, which then modifies incoming radiation, and can adjust for adiabatic changes in air temperature with elevation.

Reference weather station to estimate local air temperature and humidity

The i-Tree tools provide software utilities to process international airport weather station data, enabling global coverage. In this application, the Naples International Airport (WBAN 34113) provided the reference weather station, with its meteorological data obtained from the National Center for Environmental Information (NCEI – https://www.ncei.noaa.gov/maps/hourly/). These data were processed from their raw ISHAP format into i-Tree Cool Air inputs using the i-Tree Eco weather tool (Endreny & Hirabayashi, 2016), or alternatively the i-Tree WeatherPrep utility (https://www.itreetools.org/tools/research-suite/hydro-plus). These meteorological data represent weather for a single i-Tree Cool Air map pixel within the study domain, assigned a unique elevation, slope, aspect, tree cover, impervious cover, and land cover. As explained by Y. Yang et al. (2013), these reference station air temperature and humidity data are used in a coupled water and energy balance equations to find the air temperature and humidity at each time step for the overlying mesoscale upper boundary layer, i.e. at ~200 m above the ground using atmospheric resistances. Once the air temperature and humidity are known for the mesoscale boundary layer, the same coupled equations are then numerically solved to find the latent and sensible heat from the ground and overlying local air temperature and humidity conditions of all the other map cells in the canopy layer, i.e. 2 m above the ground. To interrogate the predictions made by the i-Tree Cool Air model, independent meteorological records were taken at five weather stations, referred to

Table 1. Codes and nomenclatures for land cover classes of the study area, according with Urban Atlas Land Use/Land Cover classification and US National Land Cover data classification. For each UA code is reported the reclassified code according to US NLCD classes.

Urban Atlas Land Use/Land Cover			United States National Land Cover Data	
Code	Nomenclature	Reclassified to NLCD Code	Code	Nomenclature
11100	Continuous Urban fabric (S.L. > 80%)	*24*	11	Open Water
11210	Discontinuous Dense Urban Fabric (S.L. 50% – 80%)	*23*	12	Perennial Ice/Snow
11220	Discontinuous Medium Density Urban Fabric (S.L. 30% – 50%)	*22*	21	Developed, Open Space
11230	Discontinuous Low Density Urban Fabric (S.L. 10% – 30%)	*21*	22	Developed, Low Intensity
11240	Discontinuous very low density urban fabric (S.L. < 10%)	*21*	23	Developed, Medium Intensity
11300	Isolated Structures	*21*	24	Developed, High Intensity
12100	Industrial, commercial, public, military and private units	*23*	31	Barren Land (Rock/Sand/Clay)
12210	Fast transit roads and associated land	*24*	43	Mixed Forest
12220	Other roads and associated land	*24*	52	Shrub/Scrub
12230	Railways and associated land	*24*	71	Grassland/Herbaceous
12300	Port areas	*24*	82	Cultivated Crops
12400	Airports	*21*		
13100	Mineral extraction and dump sites	*31*		
13300	Construction sites	*31*		
13400	Land without current use	*31*		
14100	Green urban areas	*43*		
14200	Sports and leisure facilities	*21*		
21000	Arable land (annual crops)	*82*		
22000	Permanent crops	*82*		
23000	Pastures	*71*		
31000	Forests	*43*		
32000	Herbaceous vegetation associations	*52*		
33000	Open spaces with little or no vegetations	*31*		
50000	Water	*11*		

Table 2. Monitoring weather stations in the city of Naples and related information on the position (location, latitude, longitude, elevation), type (SB: suburban background; UT: urban traffic; ST: suburban traffic), tree cover (TC), impervious cover (IMP), minimum average daily temperature (Tmin), mean average daily temperature (Tmean), and maximum average daily temperature (Tmax).

ID	Location	Latitude	Longitude	a.s.l (m)	Type	% TC	% IMP	Tmin (°C)	Tmean (°C)	Tmax (°C)
Airport	Capodichino	40°53′3.72″N	14°17′0.98″E	83	SB	0	100	17.1 ± 5	21.5 ± 4.9	25.9 ± 5.1
NA01	Osservatorio Astronomico	40°51′49.34″N	14°15′16.21″E	125	SB	0	0	18.8 ± 4.1	21.9 ± 4.2	25.5 ± 4.7
NA02	Ospedale Santobono	40°50′57.74″N	14°13′52.03″E	171	UT	0	100	19.9 ± 4.7	23.5 ± 4.9	28.4 ± 5.5
NA07	Ferrovia	40°51′15.02″N	14°16′18.17″E	13	UT	0	100	19.8 ± 4.7	23.1 ± 4.8	27.1 ± 5.1
NA08	Ospedale Pellegrini	40°52′20.40″N	14°16′31.73″E	87	ST	0	44	19 ± 4.7	22.7 ± 4.8	26.6 ± 5.1
NA09	Via Argine	40°51′49.90″N	14°20′28.94″E	36	ST	0	73	18.5 ± 4.9	22.6 ± 4.9	26.9 ± 5.1

as NA01, NA02, NA07, NA08, NA09 (see, Table 2). These stations are from the monitoring network of the regional Environmental Agency ARPA Campania (https://www.arpacampania.it/) and located within the city of Naples (Figure 1a). Precipitation data from NA01 (Supplementary 1) were integrated in the Naples International Airport to execute the model. Several heat waves occurred during the considered period (April–October 2020) according to the threshold risk for population health of the Italian heat prevention plan (www.salute.gov.it/caldo) of daily maximum apparent temperature (Tappmax) above 31°C (de'Donato et al., 2018) and showed in the figure (Supplementary 2). In this study, we did not focus on single heat waves but we considered the whole warm season.

Simulating the urban heat island and abatement with tree cover scenarios

The above inputs were combined (see Supplementary 3), and the Naples, Italy urban area was simulated with the i-Tree Cool Air model for the warm season between April and October 2020. The base case model simulation represented actual tree cover, and alternative scenarios were simulated to represent how land cover change affects hourly and daily baseline temperature and humidity, with special attention to the hottest day of the year. The two alternative scenarios are the illustrative 10% increases and decreases in tree, to cross-compare with scenarios examined by Sinha et al. (2021), and not representative of planned changes for the area. We considered for each pixel, regardless of land use class, an increase of tree cover by 10% up to max 100% and a decreasing of tree cover by 10% until min 0%. Following (Sinha et al., 2021), we considered three edge cases for tree cover (TC) and imperviousness (IMP) (0% TC – 0% IMP, 100% TC – 0% IMP, and 0% TC – 100% IMP) and interpolated hourly results of air temperature (Tair) and dew point temperature (Tdew) for intermediate TC and IMP values based on the range of each pixel (Tair and Tdew monthly average results of three edge cases are shown in the Supplementary 4–5).

Results and discussion

1) How can heat mitigation by tree cover be assessed for European cities at their full spatial extent?

Variations in temperatures within cities are primarily driven by differences in land cover variables as demonstrated in (Sinha et al., 2021, 2022), and the tree cover and impervious cover were identified as the primary land cover drivers of air temperature differences within cities (Shandas et al., 2019; Ziter et al., 2019). On this basis, the impact of the actual tree cover in Naples, proof of concept European city, was assessed coupling the i-Tree Cool Air model with CLMS UA remotely sensed land cover data accessible for major European cities. With these land cover we begin to address the question, 1) How can heat mitigation by tree cover be assessed for European cities at their full spatial extent? To answer question 1) first requires interpreting spatial patterns of CLMS UA data on tree canopy cover (Figure 1c) and impervious cover (Figure 1d). For Naples, these patterns match global patterns of urban tree cover concentrated in hills, parks, urban edges, and distant from industrial and transportation hubs or corridors (Endreny, Sica et al., 2020). The greatest tree canopy cover in Naples was concentrated at higher elevation in the northwest (see, Figure 1b), and within parks such as the Phlegraean Fields volcanic area (see green oval shape in the northwest of Figure 1c), while the impervious cover was dominant along the interior valleys, business corridors, and coastal ports. It is in these high impervious cover areas that heat wave air temperatures are likely to be greatest.

The next step in addressing question 1) was assessing land cover classes, and using those with the tree and impervious cover to predict air temperatures. This step was achieved by coupling required development of a translation between the CLMS UA land cover classes into NLCD classes required by i-Tree Cool Air, as documented in Table 1. There is no one-to-one correspondence between the land cover classes of these two remotely sensed products given CLMS UA uses a greater hierarchical classification than NLCD. For example, to describe developed, i.e. artificial, areas, the CLMS UA uses 12 classes while the NLCD uses 4 classes (e.g. 21 to 24). Following a multi-to-one maximum likelihood criterion, translation resulted in 24 UA classes (see, Figure 1e) reducing into 10 NLCD classes (see, Figure 1f), increasing cover class homogeneity across the urban area. Across Naples, the statistical distribution of NLCD classes was represented by 70% in developed land, 28% in various vegetation-covered classes (e.g. 43, 52, 71 and 82), and barren land had 2% cover (Figure 2 – Supplementary 6). The distribution of cover classes from CLMS UA follows a similar trend of most developed, followed by vegetated and barren (see, Figure 2). Furthermore, only about 8% of the urban area of Naples belong to a land cover class with a tree canopy cover (see, Figure 2) and with a degree of tree cover density ranging from 50% to 80%. About 22% of the urban surface has a tree cover density between 20% and 50%, while most of the urban area (about 70%) shows values of tree cover density less than 20%. These first results are indicative of the high rate of urbanization and the low degree of tree coverage, moreover limited to a few areas, of the city of Naples. The land cover, climatic characteristics and demographics of Naples differ greatly from those of the US cities considered in the studies from Sinha et al. (2022, 2022).

2) How much does tree cover contribute to heat mitigation in a Mediterranean city characterized by a pronounced summer drought?

To address question 2, the impact of tree cover on air temperature in Naples was assessed throughout the warm season, from April to October 2020 (Figure 3, left side), and on August 9, the hottest day of the year (Figure 3, right side). Air temperature predictions by i-Tree Cool Air for the period from April to October 2020 were organized into daily average minimum ranging from 16.1°C to 18.7°C (see, Figure 3a), daily average ranging from 19.4°C to 22.6°C (see, Figure 3b) and daily average maximum ranging from 22.7°C to 26.6°C (Figure 3c). These seasonal averages are contrasted with the predictions from 9 August 2020, with its minimum air temperature

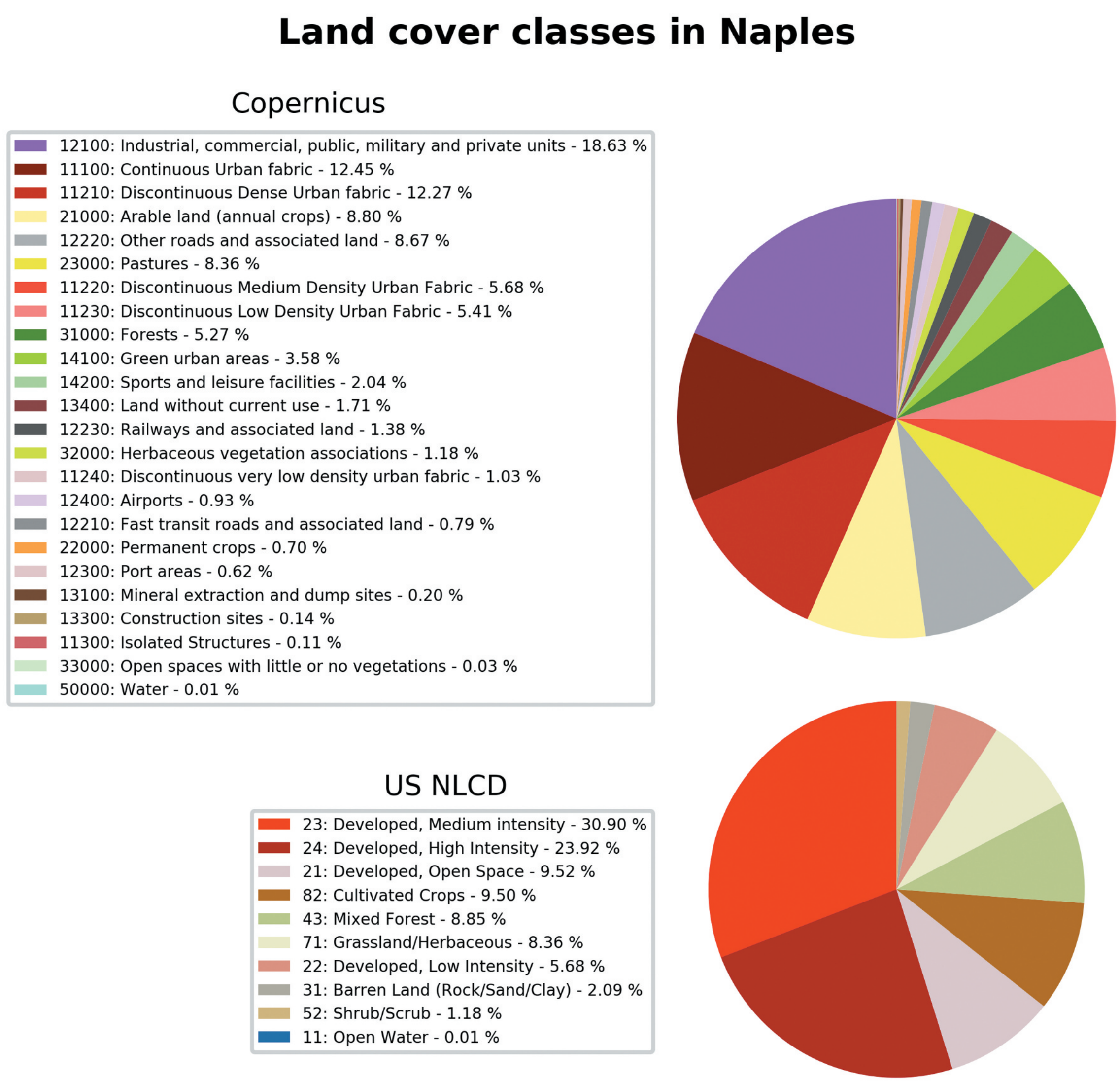

Figure 2. Percentage coverage of land use classes in the city of Naples with Copernicus (top) and US NLCD (bottom) classification.

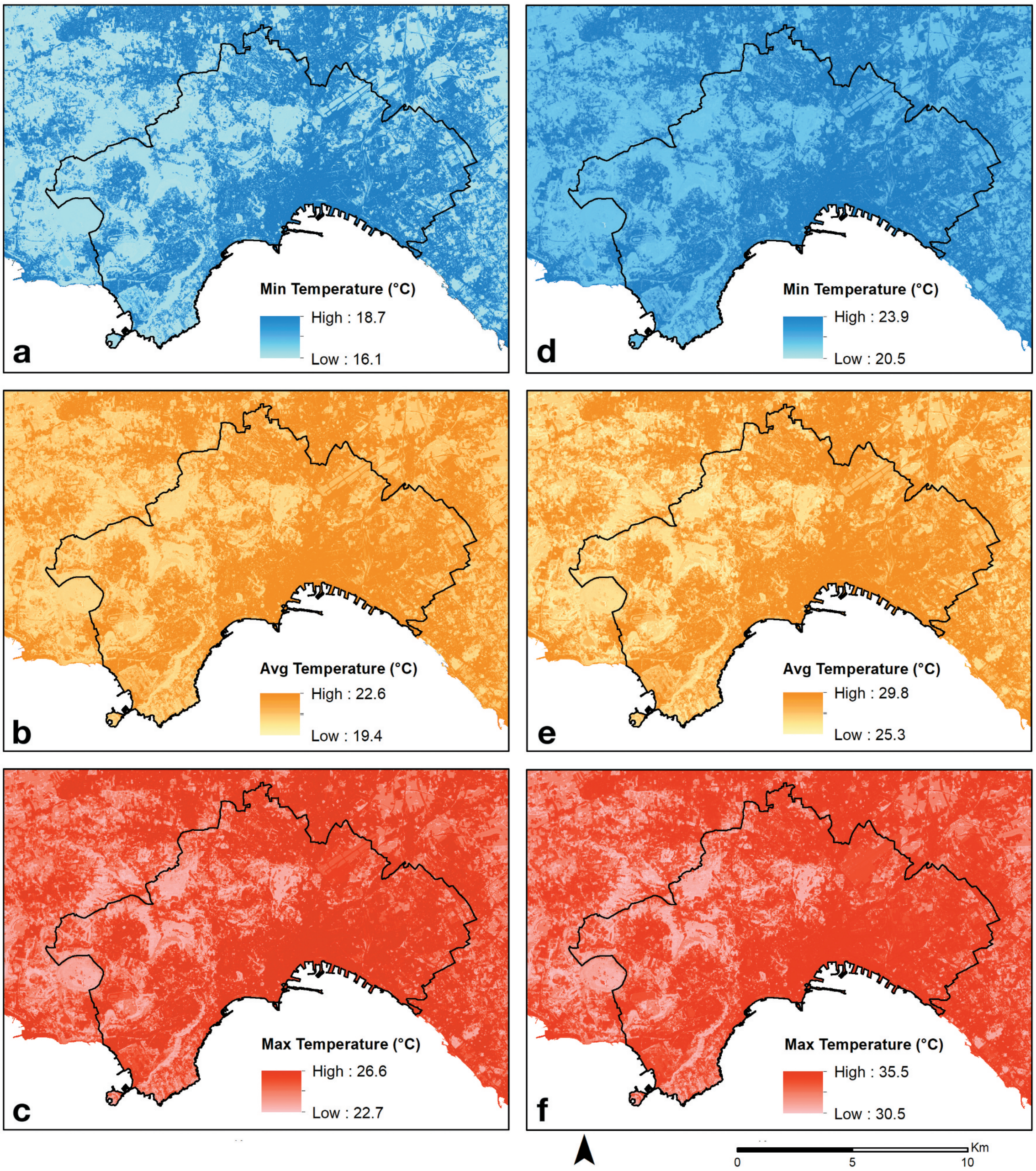

Figure 3. Left panels (a, b, c): maximum, average, and minimum daily temperature modelled with i-Tree Cool Air from April to October 2020. Right panels (d, e, f): maximum, average, and minimum hourly temperature modelled on the hottest day of the year (9 August 2020). The left and right panel of the figure show a different scale for each subplot.

spatially ranging from 20.5°C to 23.9°C (Figure 3d), average air temperature varying spatially from 25.3°C to 29.8°C (Figure 3e), and maximum air temperature spatially ranging from 30.5°C to 35.5°C (Figure 3f). The spatial pattern of these temperature ranges matches the tree cover and impervious cover spatial patterns described above, with the cooler areas congruent with the forested highlands and parks (Figure 1c), and the hotter areas overlapping the high impervious cover along the coast, its adjacent interior lands, and mixed business and residential districts radiating out to the northeast (Figure 1d). Heat mitigation by tree cover is important during the entire warm season as well as during acute events, and for minimum as well as maximum air temperatures, where high minimum temperatures can threaten night time cooling need for human health, as described by Sinha et al. (2021, 2022).

Tree cover through its evapotranspiration limited the warm season average air temperature to 19.4°C, cooler than the 22.6°C experienced on average in impervious areas (Figure 3b). Tree cover cooling effects were greater on seasonal maximum temperatures, keeping them to 22.7°C vs the 26.6°C experienced by the mostly impervious cover areas (Figure 3c). The cooling effect of tree cover was even evident in the pattern of minimum temperatures, which cooled to 16.1°C in forested areas, and rose to 18.7°C in highly impervious areas (Figure 3a). Night time minimum air temperatures in open canopy vegetated areas may drop even lower, with less resistance to airflow and promoting convective and radiative cooling (Bowler et al., 2010b). The spatial pattern and magnitude of cooler air temperature over tree canopy and hotter temperatures over impervious results similar to the observations from Wurzburg, Germany, with an average temperature gradient in summer of 1.3°C, up to 8°C of difference during extremely hot days, between the inner city sites with high impervious cover and the suburban areas with more green spaces (Rahman et al., 2022). Sinha et al. (2021) found also in Baltimore a baseline air temperature range of 2°C, averaged over April to October. Our wider 3.2°C range could be due to the particularly dense urban fabric in downtown Naples.

Of course, in assessing the effect of urban vegetation on cooling remote sensing surveys of the land surface temperature may be available and provide supporting evidence on green space reducing heat island effects (Maimaitiyiming et al., 2014). In studies of European regions, remote sensing showed relative cooling by tree cover areas up to 4°C in the southern regions, and up to 12°C cooler in central regions (Schwaab et al., 2021). The land surface temperature is greatly influenced by the shading effect of buildings and trees as reported in several studies (Lemus-Canovas et al., 2020; T. Li & Meng, 2018; C. Yang et al., 2020). The i-Tree Cool Air model simulates the air temperature and humidity assuming a flat surface representation of land cover rather than the 3D geometry of buildings and trees. The heat trapping effect on absorption of solar radiation is represented by their effective albedos (Y. Yang et al., 2013). This simplification reduces the amount and complexity of parameters to be evaluated and measured, resulting in greater computational efficiency and the possibility of applying the model in any region with 2D land cover maps. The comparison with remotely sensed about land surface temperature or vegetation-related optical indices would definitely be of interest for future research to partially evaluate the model results.

3) How reliable are the i-Tree Cool Air model estimates?

Model simulations are based on a defined parametrization per each land use class (Supplementary 3), but is unable to represent the specific boundary conditions of a single street canyon. These assumptions reduce the detailedness of the model, but allows a city-scale representation of air temperature and humidity considering the effect of different tree cover, impervious cover, and land use on urban heat. The reliability of the i-Tree Cool Air model predictions was evaluated by comparing model results with observed records from weather stations (Figures 4–6) located in different areas of the city of Naples (Figure 1a). The meteorological data recorded at the reference weather station of Naples International Airport, from April to October 2020, show values of air temperature ranging from a minimum of 7.9°C on April 1 to a maximum of 28.9°C on August 9, with a daily average of 21.5°C (Figure 4a). The dew point temperature varies from a minimum of 3.7°C on April 1 to a maximum value of 22°C on July 31 and with a daily average of 13.6°C (Figure 4a). Precipitation data, derived from NA01 weather station, indicate April as the rainiest month of 2020, while precipitations drastically decrease from May until August, with a summer drought particularly evident in July (Supplementary 1). According to climate models a longer duration of drought in the Mediterranean is predicted (Beniston et al., 2007) with higher maximum temperatures and changes in the precipitation regime (Sánchez et al., 2004), leading to climate-related extremes which can impact our study area (Bucchignani et al., 2021).

In addressing question 3, first we compared the trend of the daily average air temperature (Tair) and dew point temperature (Tdew) measured at the 5 local weather stations, over the period April – October 2020, with the respective ones of the model estimates (Figures 4b-f). The weather stations Airport (Figure 4a) and NA01 (Figure 4b) showed a lower average, respectively 21.5°C and 21.9°C, than the higher NA02 (23.5°C; Figure 4c) and NA07 (Figure 4d; 23.1°C), and intermediate NA08 (22.7°C; Figure 4d) and NA09 (22.6°C; Figure 4e). Overall, recorded Tair values are in good agreement with the modelled ones for all weather stations, while some differences exist between measured Tdew values and modelled ones.

The second step in evaluating model performance involved comparing through regression plots the predicted air temperature (Figure 5) and dew point temperature (Figure 6) with measurements recorded in the five weather stations, using hourly data. Strong correlations are observed for both air temperature ($r \geq 0.94$) and dew point temperature ($r \geq 0.89$), for all the weather stations, supporting the accuracy of the model in simulating the different land use, tree, and imperviousness conditions. These results confirm previous findings by Y. Yang et al. (2013) of a good correlation between the Tair and Tdew modelled by the i-Tree Cool Air (originally PASATH model) and weather station measurements in the city of Syracuse, NY. Some differences between model estimates and weather stations records may be due to the model not considering anthropogenic heat, which includes fuel combustion, impact of buildings and industries, and human metabolism, which can contribute upwards of 60 Wm^{-2} and a temperature increase of 1°C in summer (Sailor, 2011). The distance from highly urbanized areas, and thus possible anthropogenic heat sources, affects the air temperature. This distance

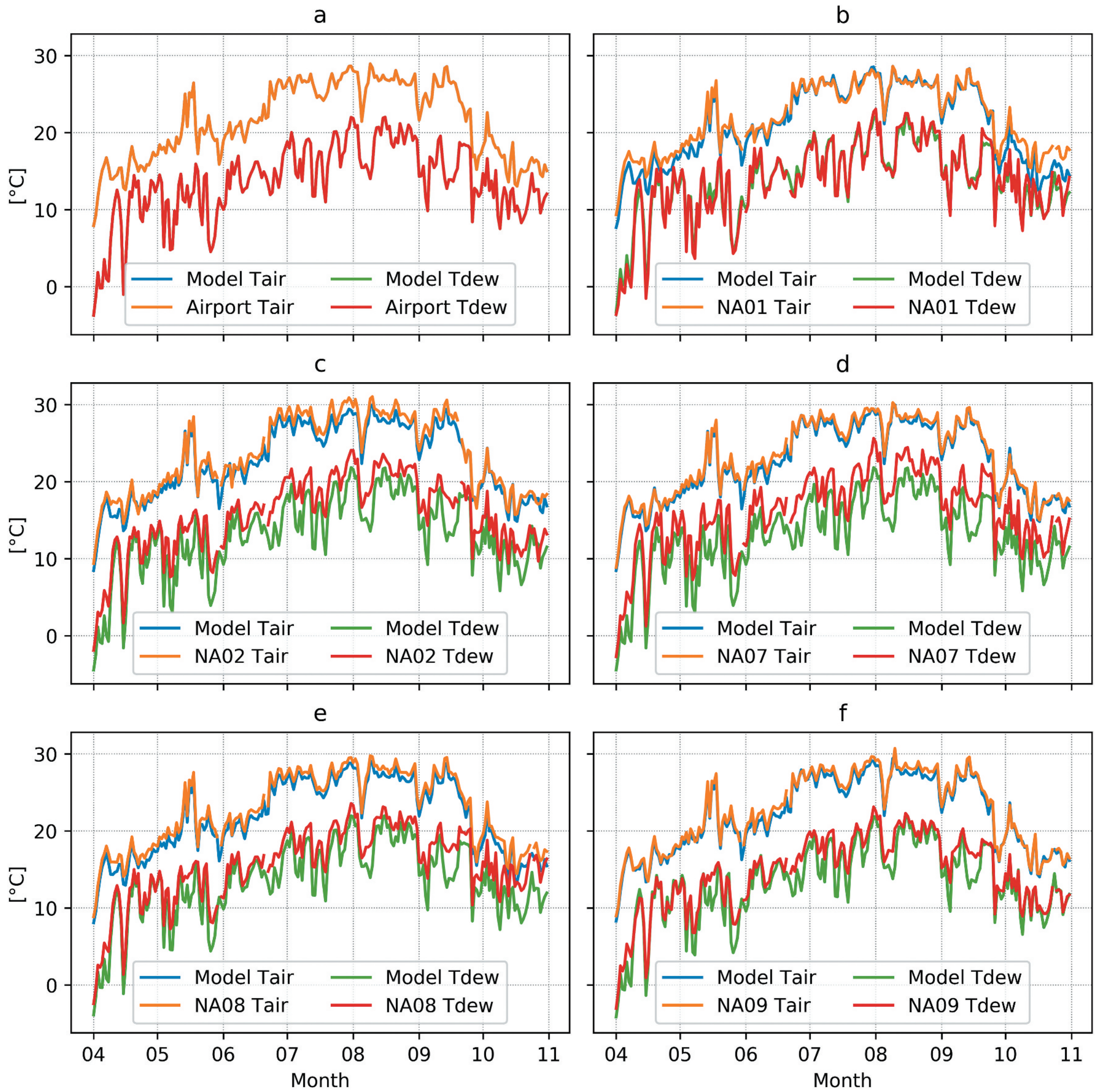

Figure 4. Modelled (blue line) vs measured (Orange line) average daily air temperature (Tair) from April to October 2020. Modelled (green line) vs measured (red line) average dew point temperature (Tdew) from April to October 2020 (weather stations – a: Airport; b: NA01; c: NA02; d: NA07; e: NA08; f: NA09). "Airport" is the reference weather station for the model.

effect is seen with the lower temperature records from stations Airport and NA01 (classified as "Suburban background (SB)"; Table 2), which sit further from developed areas. The effect of water limitations on air temperature was observed with data from station NA01, which is surrounded by vegetation; its record matched the simulated data during the driest period of simulation (Figure 4b). The stations NA02 and NA07, classified as "Urban traffic (UT)", are located in a high impervious area of the city (100% IMP; Table 2) and measured a higher average temperature. Intermediate values were recorded from NA08 and NA09, which are classified as "Suburban traffic (ST)" and show medium impervious condition (Table 2).

The percentage of tree cover or imperviousness, as well as land use, influences the urban microclimate by altering air temperature and humidity. The land cover effect on the UHI can be assessed with the i-Tree Cool Air model for virtually any scenario considered by the city. To demonstrate this point, this research examined air and dew point temperatures across the full range of potential cover, with one edge at 0% tree cover and 0% impervious cover, another edge at 100% tree cover and 0% impervious cover, and another edge at 0% tree cover and 100% impervious cover (for additional information see Supplementary 4–5). Modelled air temperature records were obtained for each edge case, and comparisons confirm that the i-Tree Cool Air model enables accurate estimates of each scenario. The magnitude of tree cover cooling varies across time, decreasing in the drier months when constrained by soil moisture deficits.

4) How much could an increase or decrease in tree cover affect heat mitigation?

The heat mitigation effect of a limited change in tree cover was assessed in model simulation scenarios for

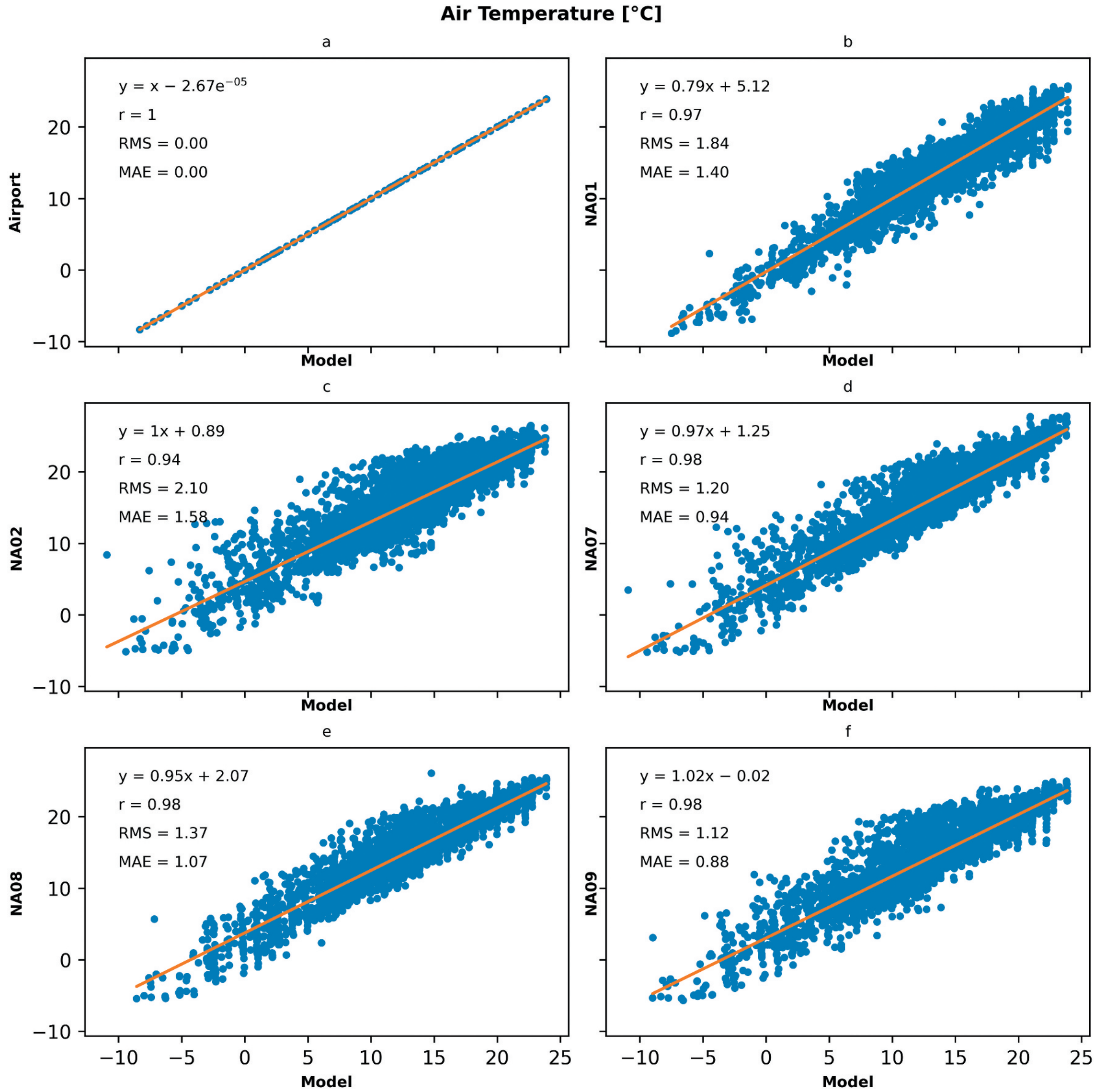

Figure 5. Comparison of hourly air temperature measured by local weather stations (a: Airport; b: NA01; c: NA02; d :NA07; e: NA08; f: NA09) and modelled with the i-Tree Cool Air from April to October 2020. "Airport" is the reference weather station for the model.

the April to October period (Figure 7) and during the August 9 heat wave (Figure 8). These scenarios limited tree cover change to a 10% increase (Figure 7–8, left side) and 10% decrease (Figure 7–8, right side) to demonstrate impacts on minimum air temperature (Figure 7–8, a-d), average air temperatures (Figure 7–8, b-e), and maximum air temperatures (Figure 7–8, c-f). We considered only a small variation because even virtuous cities like Bristol, European Green Capital Award in 2015 and with ambitious carbon neutrality targets by 2030, that planned to double the number of trees, will increase the canopy cover from 18.6% in 2018 to 37.2% by 2045 (Walters & Sinnett, 2021). We also evaluated a decreasing scenario based on the global negative trend in urban tree cover with an increase in impervious cover (Nowak & Greenfield, 2020). Increasing the tree cover by 10% resulted in an overall reduction of up to 0.2°C for maximum air temperatures (Figure 7c). The effect of increased tree cover on average air temperatures (Figure 7b) and maximum air temperature (Figure 7c) was widespread throughout the city because tree cover area is limited compared to imperviousness (Supplementary 6). The order of magnitude of air temperature reduction is comparable with results by Sinha et al. (2021). On the other hand, a decrease of tree cover by 10% generated an increase up to 0.2°C in maximum air temperature, mainly in areas with more tree cover, as the other highly urbanized areas already lack it and show no change (Figure 7e-f). No changes were shown for the minimum temperature with these limited changes in tree cover (Figure 7a, d).

The impact on air temperatures of changes in tree cover was also examined for the hottest day of the season, 9 August 2020. Minimum air temperature fell slightly with a 10% increase in tree cover (Figure 8a), and a rose slightly with a 10% decrease in tree cover (Figure 8d). The spatial distribution of changes in air temperatures was similar between the descriptive statistics of average (Figure 8b) and maximum

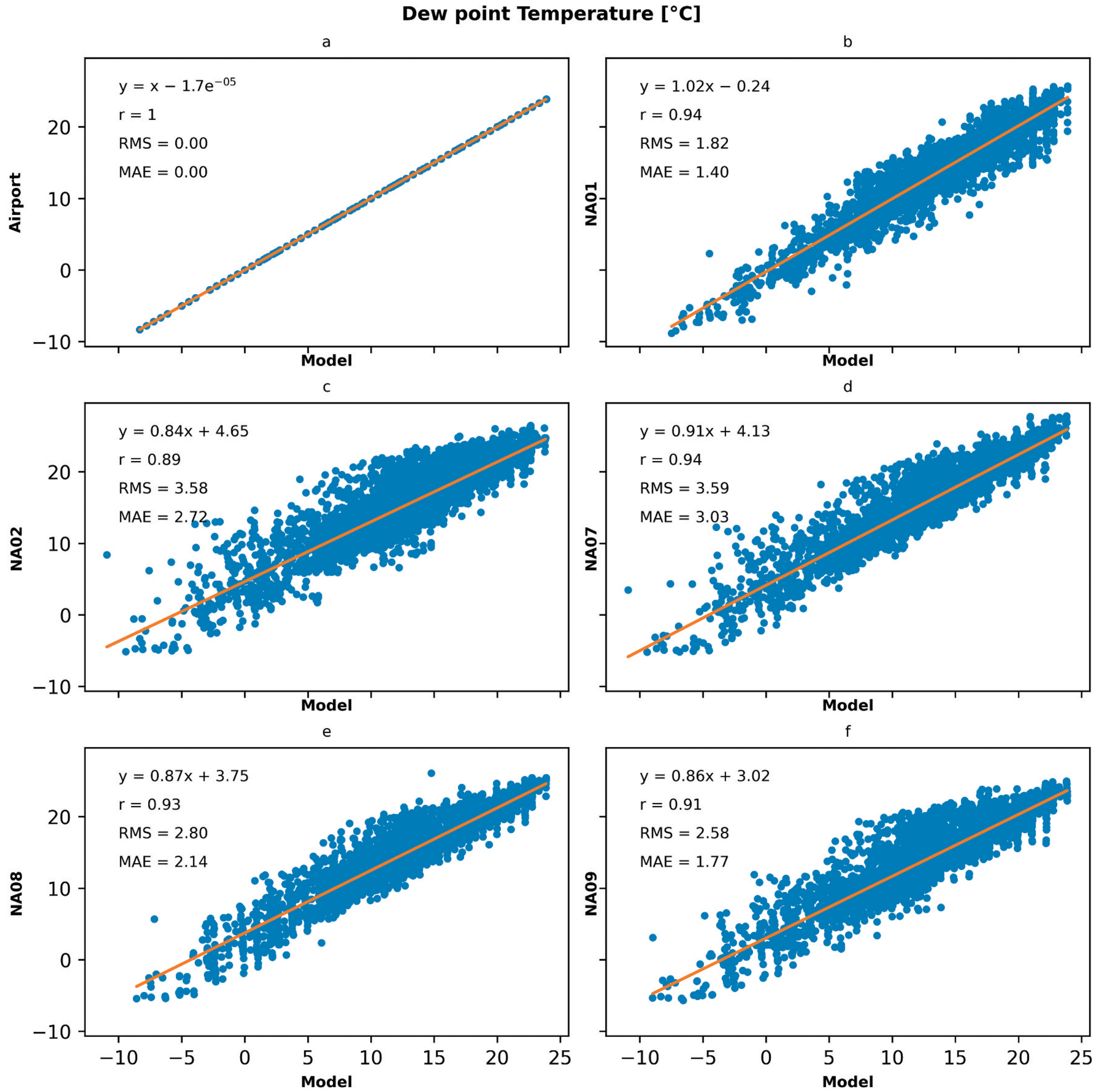

Figure 6. Comparison of hourly dew point temperature measured by local weather stations (a: Airport; b: NA01; c: NA02; d: NA07; e: NA08; f: NA09) and modelled with the i-Tree Cool Air from April to October 2020. "Airport" is the reference weather station for the model.

(Figure 8c). Clearly, urbanized areas benefit from an increase in tree cover given this leads to lower extreme temperatures during heat waves. The 10% loss of tree cover lead increased the air temperature statistics of minimum (Figure 8d), average (Figure 8e) and maximum (Figure 8f), with increasing variability for maximum temperature changes.

From a temporal perspective, the cooling impact of increased tree cover is greatest in the spring months when the water balance is positive due to rainfall (Supplementary 1), then decreases abruptly in the summer months due to the severe drought, and rises again in October (an opposite effect in the case of −10% tree coverage; Figure 9). These results highlight the importance of the cooling effect related to tree evapotranspiration in urban heat mitigation, which contributes significantly to latent heat flux and thus to air temperature reduction (Liu et al., 2017; Smith et al., 2021). Conversely, Sinha et al. (2021) show a maximum temperature reduction in July from urban tree canopy in Baltimore, showing how a different precipitation regime affects the cooling effect of trees. On the other, soil drought negatively impacts the water balance of the vegetation reducing evapotranspiration (Teskey et al., 2015) and thus limiting the cooling effect on temperature mitigation (Pace et al., 2021).

5) How can these results support urban planning?

To understand how much and where tree cover can support heat mitigation in the city, we evaluated the effect on temperature change for the two scenarios, 10% gain and loss of tree cover (Figure 10). The scenarios, in light of the reforestation policies of many cities, aimed to highlight how the impact of tree cover can reduce urban heat especially in the

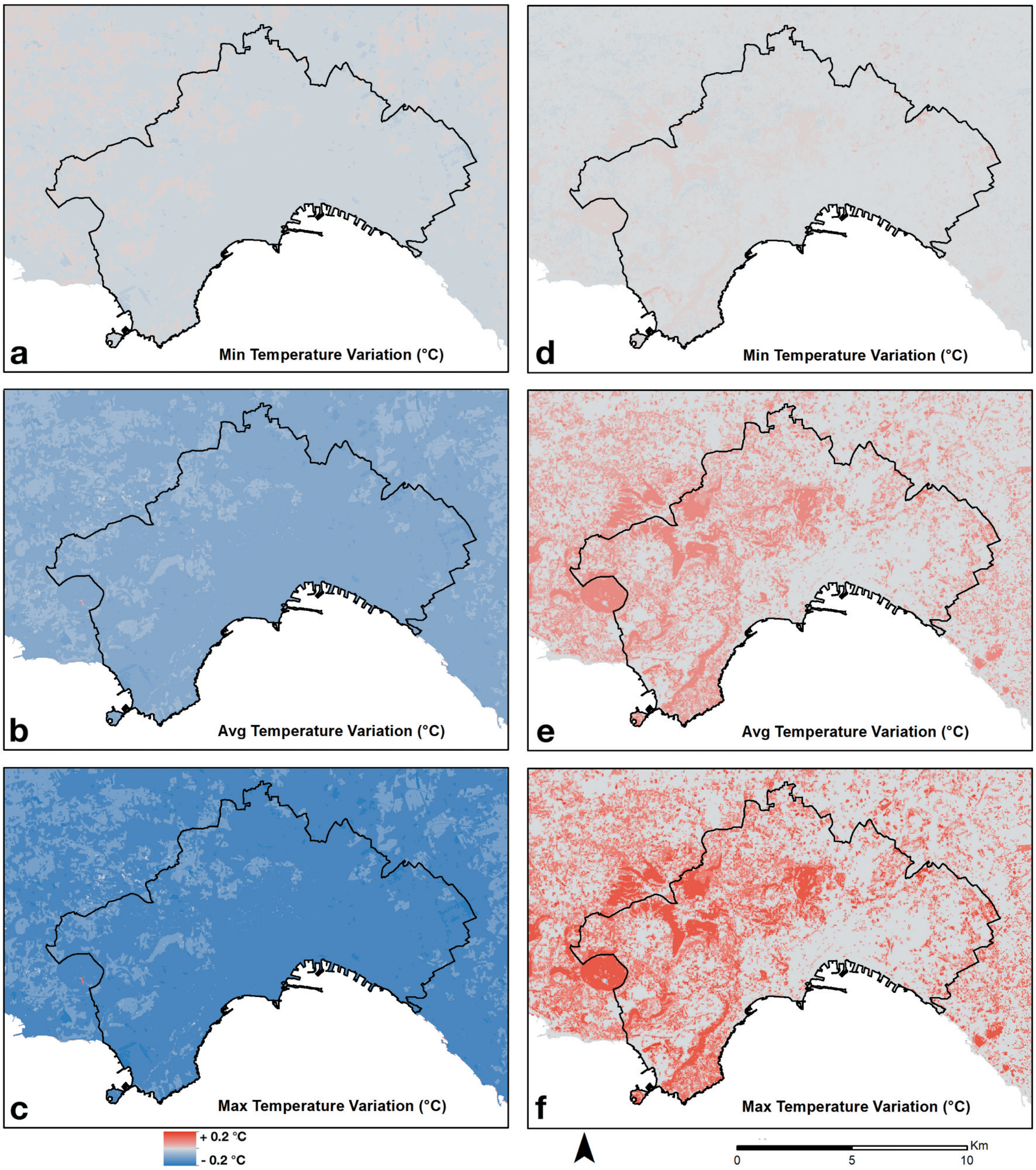

Figure 7. From top to bottom: minimum, average, and maximum daily temperature reduction averaged from April to October 2020, increasing (left) and decreasing (right) tree cover by 10%.

most urbanized areas, which often lack tree cover, and at the same time the importance of preserving existing urban forests. The largest impact on air temperature of increasing tree cover occurred in urbanized areas (NLCD classes 21 to 24) and areas without vegetation (NLCD class 31), while the greatest impact of reducing tree cover occurred in vegetated areas (NLCD classes 43, 52, 71, 81) and particularly forest (NLCD class 43; Figure 10). This suggests that if the goal is to cool the city, tree planting and other vegetative greening should likely focus on the densely urbanized areas of the city, while preserving all existing urban forests that play an important role in temperature mitigation. The selection of tree species with high cooling potential (Rahman et al., 2020) and capable of withstanding heat waves and extreme drought will be essential to ensure plant growth and other ecosystem services such as temperature mitigation (Rötzer et al., 2021). Solutions that use rainwater runoff such as passive irrigation systems can increase growth and transpiration by limiting drought stress (Thom et al., 2022). Renewable electricity for urban dwellers, e.g. to charge a portable device while in the park, can also be powered by this mix of stormwater and plant roots using a new technology called microbial fuel cells that are situated in the soil (Endreny, Avignone-Rossa et al., 2020). Trees effectively contribute to temperature mitigation through both shade and evapotranspiration, however in heavily urbanized cities such as Naples, the lack of space to plant new trees is

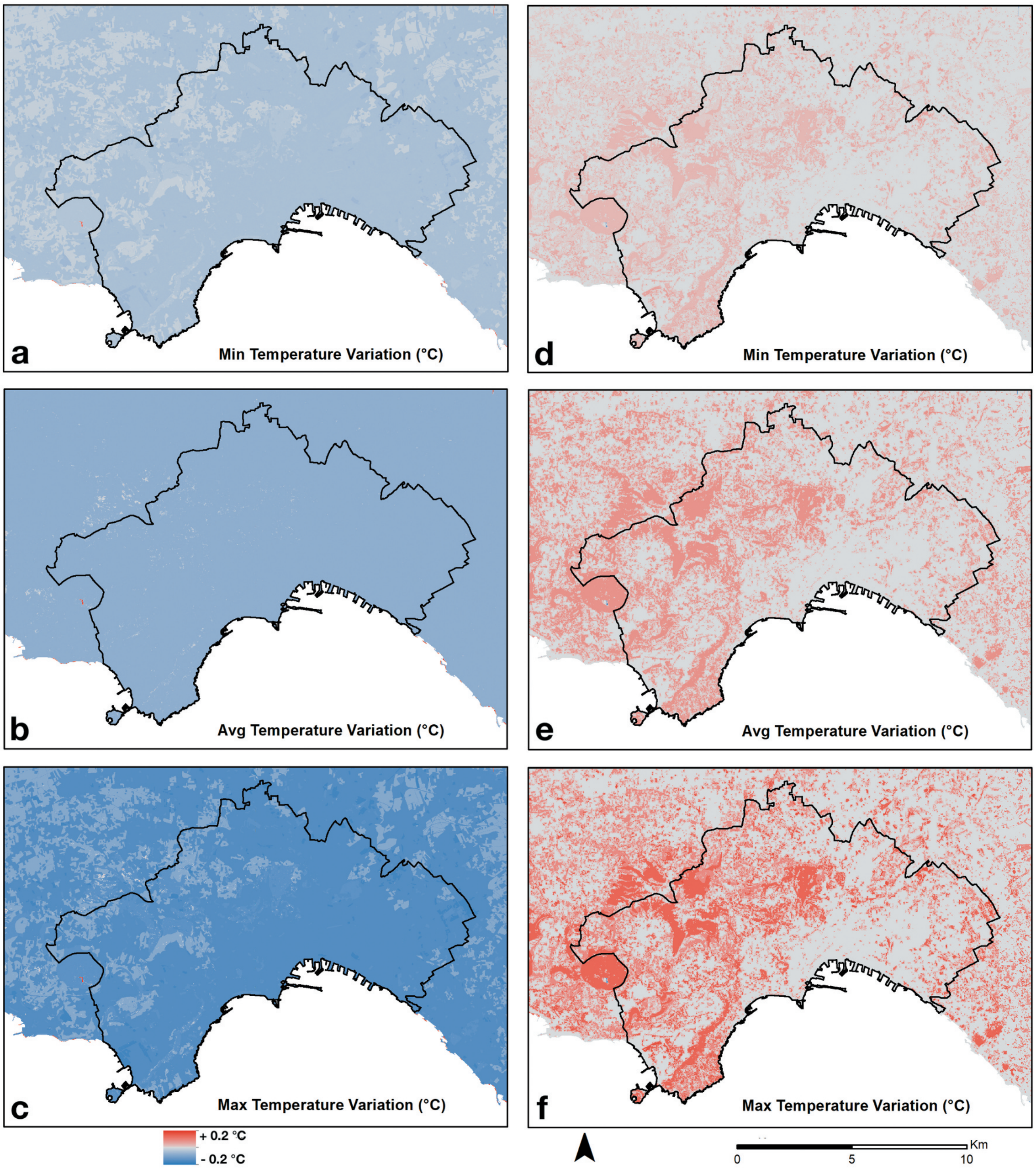

Figure 8. From top to bottom: minimum, average, and maximum hourly temperature reduction on the hottest day of the year (9 August 2020), increasing (left) and decreasing (right) tree cover by 10%.

a major obstacle that could be partially offset by the use of green infrastructure such as green roofs (Rowe & Getter, 2006) or green walls (Susca et al., 2022).

Conclusions

In this study we developed a suitable methodology for European cities to simulate heat wave vulnerability and nature-based solutions using freely available Copernicus data within the i-Tree Cool Air model. Specifically, the research established a method for converting Copernicus Urban Atlas estimates of land cover class into the Anderson level 2 format used by the i-Tree Cool Air model, and extracted tree canopy and impervious cover values. This methodology was demonstrated for the city of Naples, Italy, characterized by a pronounced Mediterranean climate with hot and dry summers, creating a proof of concept. The approach yielded a strong correlation between predicted and observed air and dew point temperature using local weather stations across the city, demonstrating the reliability of the model.

Air temperature maps generated with model output for a 2020 heat wave graphically captured a 5°C difference in air temperature between urban forested areas and urbanized impervious areas, highlighting the significant heat abatement function of trees for city and regional planners. The cooling offered by trees during heat waves was constrained by low soil water content, caused by lack of precipitation, suggesting irrigation of trees may be strategic to maximize

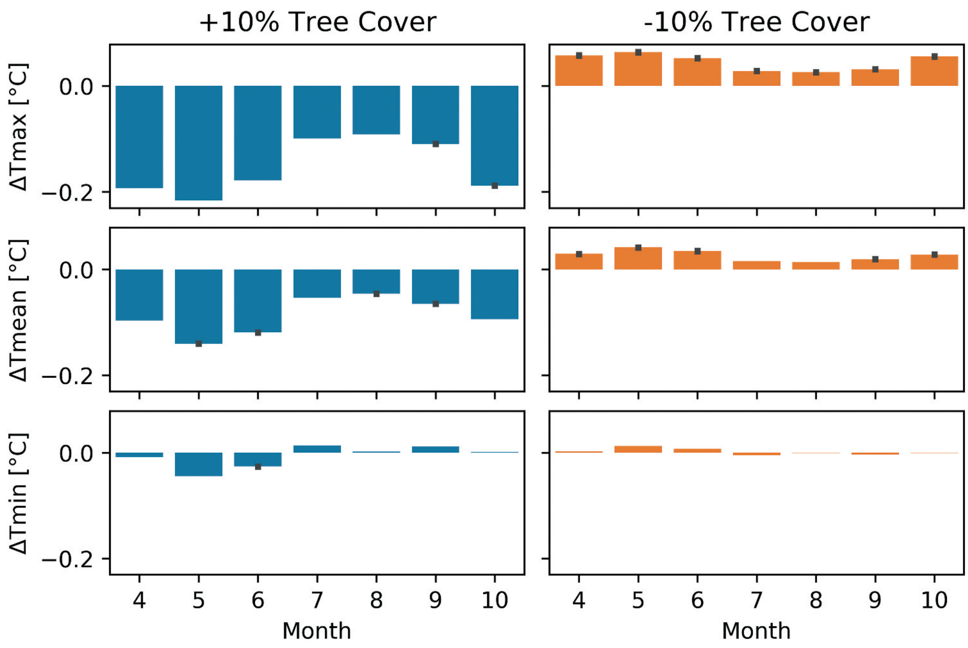

Figure 9. Monthly variation in maximum, average, and minimum temperature from April to October 2020, increasing tree cover by 10% (left) and decreasing by 10% (right).

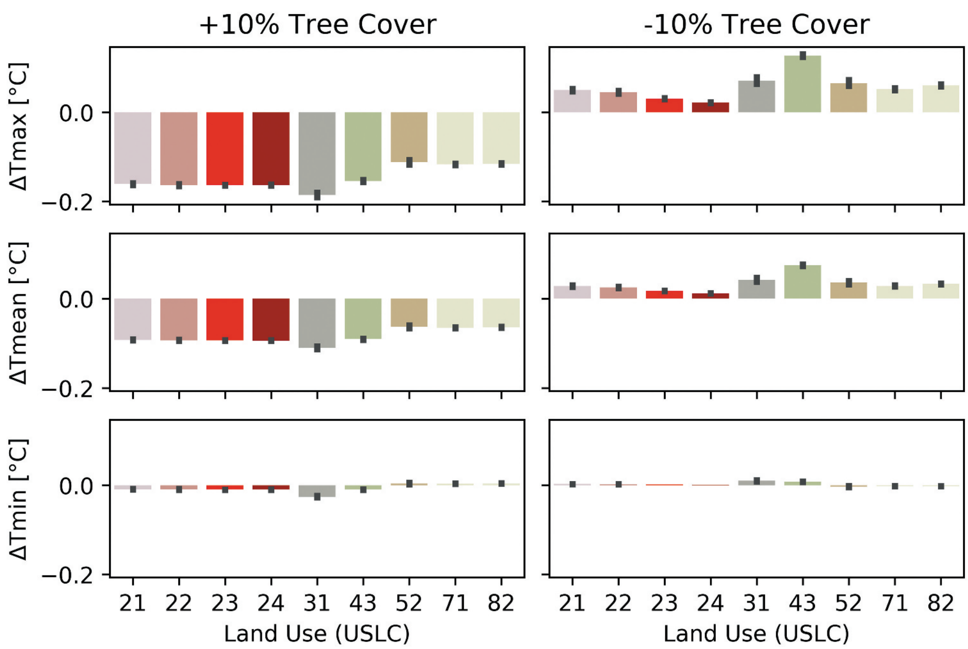

Figure 10. Monthly variation in maximum, average, and minimum temperature per each land use class from April to October 2020, increasing tree cover by 10% (left) and decreasing by 10% (right) [Land use classes – 21: Developed, Open Space; 22: Developed, Low Intensity, 23: Developed, Medium intensity, 24: Developed, High Intensity, 31: Barren Land (Rock/Sand/Clay), 43: Mixed Forest, 52: Shrub/Scrub, 71: Grassland/Herbaceous, 82: Cultivated Crops].

cooling benefits. The model simulated potential tree cover scenarios, showing a 10% increase in tree cover can reduce air temperature by 0.2°C, noting additional cooling is obtained by removing impervious cover. Conversely, a tree cover loss of 10% can cause an increase in temperature especially in areas with higher tree density, highlighting the need to preserve these areas to maintain the urban microclimate. City and regional planners can use remotely sensed land cover data within this mechanistic i-Tree Cool Air model to strategically design tree planting and increase community resilience to the impact of climate change and the exacerbation of heat waves.

Acknowledgments

This research was supported by the project "EUFORICC" – Establishing Urban Forest based solutions In Changing Cities (PRIN 20173RRN2S: "Projects of National Interest"). R. Pace was also supported by the project

'Grüne Lunge 2.0', funded by the Federal Ministry of Education and Research (BMBF, 01LR2015A), Germany. T. Endreny was supported by NUCFAC project 21-DG -11094200-242 for increasing community resilience via urban forest planning. The authors would like to thank Robert C. Coville and Jay Heppler for their assistance with i-Tree tools.

Disclosure statement

No potential conflict of interest was reported by the author(s).

ORCID

Rocco Pace http://orcid.org/0000-0002-3126-635X
Francesca Chiocchini http://orcid.org/0000-0002-5122-8756
Maurizio Sarti http://orcid.org/0000-0002-5063-4154
Theodore A. Endreny http://orcid.org/0000-0002-1891-261X
Carlo Calfapietra http://orcid.org/0000-0001-5040-4343
Marco Ciolfi http://orcid.org/0000-0003-4831-8053

References

Baldwin, J. W., Dessy, J. B., Vecchi, G. A., & Oppenheimer, M. (2019). Temporally compound heat wave events and global warming: An emerging hazard. *Earth's Future*, *7*(4), 411–427. https://doi.org/10.1029/2018EF000989

Beniston, M., Stephenson, D. B., Christensen, O. B., Ferro, C. A. T., Frei, C., Goyette, S., Halsnaes, K., Holt, T., Jylhä, K., Koffi, B., Palutikof, J., Schöll, R., Semmler, T., & Woth, K. (2007). Future extreme events in European climate: An exploration of regional climate model projections. *Climatic Change*, *81*(SUPPL. 1), 71–95. https://doi.org/10.1007/s10584-006-9226-z

Bowler, D. E., Buyung-Ali, L., Knight, T. M., & Pullin, A. S. (2010a). Urban greening to cool towns and cities: A systematic review of the empirical evidence. *Landscape and Urban Planning*, *97*(3), 147–155. https://doi.org/10.1016/j.landurbplan.2010.05.006

Bowler, D. E., Buyung-Ali, L., Knight, T. M., & Pullin, A. S. (2010b). Urban greening to cool towns and cities: A systematic review of the empirical evidence. *Landscape and Urban Planning*, *97*(3), 147–155. https://doi.org/10.1016/j.landurbplan.2010.05.006

Bucchignani, E., Zollo, A. L., & Montesarchio, M. (2021). Analysis of expected climate extreme variability with regional climate simulations over Napoli Capodichino Airport: A contribution to a climate risk assessment framework. *Earth*, *2*(4), 980–996. https://doi.org/10.3390/earth2040058

Buccolieri, R., Santiago, J. L., Rivas, E., & Sanchez, B. (2018). Review on urban tree modelling in CFD simulations: Aerodynamic, deposition and thermal effects. *Urban Forestry and Urban Greening*, *31*, 212–220. https://doi.org/10.1016/j.ufug.2018.03.003

Cadenasso, M. L., Pickett, S. T. A., & Schwarz, K. (2007). Spatial heterogeneity in urban ecosystems: Reconceptualizing land cover and a framework for classification. *Frontiers in Ecology and the Environment*, *5*(2), 80–88. https://doi.org/10.1890/1540-9295(2007)5[80:SHIUER]2.0.CO;2

de'Donato, F., Scortichini, M., de Sario, M., de Martino, A., & Michelozzi, P. (2018). Temporal variation in the effect of heat and the role of the Italian heat prevention plan. *Public Health*, *161*, 154–162. https://doi.org/10.1016/j.puhe.2018.03.030

Endreny, T. A., Avignone-Rossa, C., & Nastro, R. A. (2020). Generating electricity with urban green infrastructure microbial fuel cells. *Journal of Cleaner Production*, *263*, 121337. https://doi.org/10.1016/j.jclepro.2020.121337

Endreny, T. A., Sica, F., & Nowak, D. J. (2020). Tree cover is unevenly distributed across cities globally, with lowest levels near highway pollution sources. *Frontiers in Sustainable Cities* 2, 16. https://doi.org/10.3389/frsc.2020.00016

Founda, D., Pierros, F., Petrakis, M., & Zerefos, C. (2015). Interdecadal variations and trends of the Urban Heat Island in Athens (Greece) and its response to heat waves. *Atmospheric Research*, *161–162*, 1–13. https://doi.org/10.1016/j.atmosres.2015.03.016

Gatto, E., Buccolieri, R., Perronace, L., & Santiago, J. L. (2021). The challenge in the management of historic trees in urban environments during climate change: The case of corso trieste (Rome, Italy). *Atmosphere*, *12*(4), 500. https://doi.org/10.3390/atmos12040500

Guerreiro, S. B., Dawson, R. J., Kilsby, C., Lewis, E., & Ford, A. (2018). Future heat-waves, droughts and floods in 571 European cities. *Environmental Research Letters*, *13*(3), 034009. https://doi.org/10.1088/1748-9326/aaaad3

Guo, Y., Gasparrini, A., Li, S., Sera, F., Vicedo-Cabrera, A. M., de Sousa Zanotti Stagliorio Coelho, M., Saldiva, P. H. N., Lavigne, E., Tawatsupa, B., Punnasiri, K., Overcenco, A., Correa, P. M., Ortega, N. V., Kan, H., Osorio, S., Jaakkola, J. J. K., Ryti, N. R. I., Goodman, P. G., Zeka, A., . . . Michelozzi, P. (2018). Quantifying excess deaths related to heatwaves under climate change scenarios: A multicountry time series modelling study. *PLoS Medicine*, *15*(7), 1–17. https://doi.org/10.1371/journal.pmed.1002629

Haines, A., Kovats, R., Campbell-Lendrum, D., & Corvalan, C. (2006). Climate change and human health: Impacts, vulnerability, and mitigation. *Lancet*, *367*(9528), 2101–2109. https://doi.org/10.1016/S0140-6736(06)68933-2

He, B. J., Wang, J., Liu, H., & Ulpiani, G. (2021). Localized synergies between heat waves and urban heat islands: Implications on human thermal comfort and urban heat management. *Environmental Research*, *193*, 110584. https://doi.org/10.1016/j.envres.2020.110584

Hirabayashi, S., & Endreny, T. A. (2016). Surface and Upper Weather Pre-processor for i-Tree Eco and Hydro. 20 09 2022. https://www.itreetools.org/documents/554/Surface_and_Upper_Weather_Pre-processor_Description.pdf

ISTAT. (2021a). *Bilancio demografico anno 2021*. https://demo.istat.it/bilmens/query.php?lingua=ita&Rip=S4&Reg=R15&Pro=P063&Com=49&anno=2021&submit=Tavola

ISTAT. (2021b). *Temperatura e precipitazione nelle città capoluogo di regione e città metropolitane - anno 2020 e serie storica 2010-2020*. https://www.istat.it/it/archivio/263811

Klok, L., Zwart, S., Verhagen, H., & Mauri, E. (2012). The surface heat island of Rotterdam and its relationship with urban surface characteristics. *Resources, Conservation and Recycling*, *64*, 23–29. https://doi.org/10.1016/j.resconrec.2012.01.009

Konarska, J., Uddling, J., Holmer, B., Lutz, M., Lindberg, F., Pleijel, H., & Thorsson, S. (2016). Transpiration of urban trees and its cooling effect in a high latitude city. *International Journal of Biometeorology*, *60*(1), 159–172. https://doi.org/10.1007/s00484-015-1014-x

Krayenhoff, E. S., Christen, A., Martilli, A., & Oke, T. R. (2014). A multi-layer radiation model for urban neighbourhoods with trees. *Boundary-Layer Meteorology*, *151* (1), 139–178. https://doi.org/10.1007/s10546-013-9883-1

Lee, S. H., & Park, S. U. (2008). A vegetated urban canopy model for meteorological and environmental modelling. *Boundary-Layer Meteorology*, *126*(1), 73–102. https://doi.org/10.1007/s10546-007-9221-6

Lemus-Canovas, M., Martin-Vide, J., Moreno-Garcia, M. C., & Lopez-Bustins, J. A. (2020). Estimating Barcelona's metropolitan daytime hot and cold poles using landsat-8 land surface temperature. *Science of the Total Environment* 699, 134307. https://doi.org/10.1016/j.scitotenv.2019.134307

Li, D., & Bou-Zeid, E. (2013). Synergistic interactions between urban heat islands and heat waves: The impact in cities is larger than the sum of its parts. *Journal of Applied Meteorology and Climatology*, *52*(9), 2051–2064. https://doi.org/10.1175/JAMC-D-13-02.1

Li, T., & Meng, Q. (2018). A mixture emissivity analysis method for urban land surface temperature retrieval from Landsat 8 data. *Landscape and Urban Planning*, *179*, 63–71. https://doi.org/10.1016/j.landurbplan.2018.07.010

Liu, X., Li, X. X., Harshan, S., Roth, M., & Velasco, E. (2017). Evaluation of an urban canopy model in a tropical city: The role of tree evapotranspiration. *Environmental Research Letters*, *12*(9), 094008. https://doi.org/10.1088/1748-9326/aa7ee7

Maimaitiyiming, M., Ghulam, A., Tiyip, T., Pla, F., Latorre-Carmona, P., Halik, Ü., Sawut, M., & Caetano, M. (2014). Effects of green space spatial pattern on land surface temperature: Implications for sustainable urban planning and climate change adaptation. *ISPRS Journal of Photogrammetry and Remote Sensing*, *89*, 59–66. https://doi.org/10.1016/j.isprsjprs.2013.12.010

Massetti, L., Petralli, M., Napoli, M., Brandani, G., Orlandini, S., & Pearlmutter, D. (2019). Effects of deciduous shade trees on surface temperature and pedestrian thermal stress during summer and autumn. *International Journal of Biometeorology*, *63*(4), 467–479. https://doi.org/10.1007/s00484-019-01678-1

McGeehin, M. A., & Mirabelli, M. (2001). The potential impacts of climate variability and change on temperature-related morbidity and mortality in the United States. *Environmental Health Perspectives*, *109*(suppl 2), 185–189. https://doi.org/10.1289/ehp.109-1240665

Meehl, G. A., & Tebaldi, C. (2004). More intense, more frequent, and longer lasting heat waves in the 21st century. *Science*, *305*(5686), 994–997. https://doi.org/10.1126/science.1098704

Meier, F., & Scherer, D. (2012). Spatial and temporal variability of urban tree canopy temperature during summer 2010 in Berlin, Germany. *Theoretical and Applied Climatology*, *110*(3), 373–384. https://doi.org/10.1007/s00704-012-0631-0

Ngarambe, J., Nganyiyimana, J., Kim, I., Santamouris, M., & Young Yun, G. (2020). Synergies between urban heat island and heat waves in Seoul: The role of wind speed and land use characteristics. *PLoS ONE 15*(12) e0243571 . https://doi.org/10.1371/journal.pone.0243571 .

Norton, B. A., Coutts, A. M., Livesley, S. J., Harris, R. J., Hunter, A. M., & Williams, N. S. G. (2015). Planning for cooler cities: A framework to prioritise green infrastructure to mitigate high temperatures in urban landscapes. *Landscape and Urban Planning*, *134*, 127–138. https://doi.org/10.1016/j.landurbplan.2014.10.018

Nowak, D. J., & Greenfield, E. J. (2020). The increase of impervious cover and decrease of tree cover within urban areas globally (2012–2017). *Urban Forestry and Urban Greening* 49, 126638. https://doi.org/10.1016/j.ufug.2020.126638

Oliveira, S., Andrade, H., & Vaz, T. (2011). The cooling effect of green spaces as a contribution to the mitigation of urban heat: A case study in Lisbon. *Building and Environment*, *46*(11), 2186–2194. https://doi.org/10.1016/j.buildenv.2011.04.034

Pace, R., De Fino, F., Rahman, M. A., Pauleit, S., Nowak, D. J., & Grote, R. (2021). A single tree model to consistently simulate cooling, shading, and pollution uptake of urban trees. *International Journal of Biometeorology*, *65*(2), 277–289. https://doi.org/10.1007/s00484-020-02030-8

Rahman, M. A., Franceschi, E., Pattnaik, N., Moser-Reischl, A., Hartmann, C., Paeth, H., Pretzsch, H., Rötzer, T., & Pauleit, S. (2022). Spatial and temporal changes of outdoor thermal stress: Influence of urban land cover types. *Scientific Reports*, *12*(1), 671. https://doi.org/10.1038/s41598-021-04669-8

Rahman, M. A., Moser, A., Rötzer, T., & Pauleit, S. (2017). Within canopy temperature differences and cooling ability of Tilia cordata trees grown in urban conditions. *Building and Environment*, *114*, 118–128. https://doi.org/10.1016/j.buildenv.2016.12.013

Rahman, M. A., Stratopoulos, L. M. F., Moser-Reischl, A., Zölch, T., Häberle, K. H., Rötzer, T., Pretzsch, H., & Pauleit, S. (2020). Traits of trees for cooling urban heat islands: A meta-analysis. *Building and Environment*, *170*, 106606. https://doi.org/10.1016/j.buildenv.2019.106606

Rahmstorf, S., & Coumou, D. (2011). Increase of extreme events in a warming world. *Proceedings of the National Academy of Sciences*, *108*(44), 17905–17909. https://doi.org/10.1073/pnas.1101766108

Redon, E., Lemonsu, A., & Masson, V. (2020). An urban trees parameterization for modeling microclimatic variables and thermal comfort conditions at street level with the Town Energy Balance model (TEB-SURFEX v8.0). *Geoscientific Model Development*, *13*(2), 385–399. https://doi.org/10.5194/gmd-13-385-2020

Rizvi, S. H., Alam, K., & Iqbal, M. J. (2019). Spatio -temporal variations in urban heat island and its interaction with heat wave. *Journal of Atmospheric and Solar-Terrestrial Physics*, *185*, 50–57. https://doi.org/10.1016/j.jastp.2019.02.001

Robine, J. M., Cheung, S. L. K., Le Roy, S., Van Oyen, H., Griffiths, C., Michel, J. P., & Herrmann, F. R. (2008). Death toll exceeded 70,000 in Europe during the summer of 2003. *Comptes Rendus - Biologies*, *331*(2), 171–178. https://doi.org/10.1016/j.crvi.2007.12.001

Rötzer, T., Moser-Reischl, A., Rahman, M. A., Hartmann, C., Paeth, H., Pauleit, S., & Pretzsch, H. (2021). Urban tree growth and ecosystem services under extreme drought. *Agricultural and Forest Meteorology*, *308–309*, 108532. https://doi.org/10.1016/j.agrformet.2021.108532

Rötzer, T., Rahman, M. A., Moser-Reischl, A., Pauleit, S., & Pretzsch, H. (2019). Process based simulation of tree growth and ecosystem services of urban trees under present and future climate conditions. *Science of the Total Environment*, *676*, 651–664. https://doi.org/10.1016/j.scitotenv.2019.04.235

Rowe, D. B., & Getter, K. L. (2006). The role of extensive green roofs in sustainable development. *HortScience*, *41*(5), 1276–1285. https://doi.org/10.21273/HORTSCI.41.5.1276

Russo, S., Dosio, A., Graversen, R. G., Sillmann, J., Carrao, H., Dunbar, M. B., Singleton, A., Montagna, P., Barbola, P., & Vogt, J. V. (2014). Magnitude of extreme heat waves in present climate and their projection in a warming world. *Journal of Geophysical Research Atmospheres*, *119*(22), 12–500. https://doi.org/10.1002/2014JD022098

Sailor, D. J. (2011). A review of methods for estimating anthropogenic heat and moisture emissions in the urban environment. *International Journal of Climatology*, *31* (2), 189–199. https://doi.org/10.1002/joc.2106

Sánchez, E., Gallardo, C., Gaertner, M. A., Arribas, A., & Castro, M. (2004). Future climate extreme events in the Mediterranean simulated by a regional climate model: A first approach. *Global and Planetary Change*, *44*(1–4), 163–180. https://doi.org/10.1016/j.gloplacha.2004.06.010

Schwaab, J., Meier, R., Mussetti, G., Seneviratne, S., Bürgi, C., & Davin, E. L. (2021). The role of urban trees in reducing land surface temperatures in European cities. *Nature Communications*, *12*(1), 1–11. https://doi.org/10.1038/s41467-021-26768-w

Shandas, V., Voelkel, J., Williams, J., & Hoffman, J. (2019). Integrating satellite and ground measurements for predicting locations of extreme urban heat. *Climate*, *7*(1), 1–13. https://doi.org/10.3390/cli7010005

Sinha, P., Coville, R. C., Hirabayashi, S., Lim, B., Endreny, T. A., & Nowak, D. J. (2021). Modeling lives saved from extreme heat by urban tree cover☆. *Ecological Modelling*, *449*, 109553. https://doi.org/10.1016/j.ecolmodel.2021.109553

Sinha, P., Coville, R. C., Hirabayashi, S., Lim, B., Endreny, T. A., & Nowak, D. J. (2022). Variation in estimates of heat-related mortality reduction due to tree cover in U.S. cities. *Journal of Environmental Management*, *301*, 113751. https://doi.org/10.1016/j.jenvman.2021.113751

Smith, I. A., Winbourne, J. B., Tieskens, K. F., Jones, T. S., Bromley, F. L., Li, D., & Hutyra, L. R. (2021). A satellite-based model for estimating latent heat flux from urban vegetation. *Frontiers in Ecology and Evolution*, *9*, 695995. https://doi.org/10.3389/fevo.2021.695995

Sobrino, J. A., Oltra-Carrió, R., Sòria, G., Bianchi, R., & Paganini, M. (2012). Impact of spatial resolution and satellite overpass time on evaluation of the surface urban heat island effects. *Remote Sensing of Environment*, *117*, 50–56. https://doi.org/10.1016/j.rse.2011.04.042

Speak, A., Montagnani, L., Wellstein, C., & Zerbe, S. (2020). The influence of tree traits on urban ground surface shade cooling. *Landscape and Urban Planning*, *197*, 103748. https://doi.org/10.1016/j.landurbplan.2020.103748

Susca, T., Zanghirella, F., Colasuonno, L., & Fatto, V. D. (2022). Effect of green wall installation on urban heat island and building energy use : A climate-informed systematic literature review. *Renewable and Sustainable Energy Reviews*, *159*, 112100. https://doi.org/10.1016/j.rser.2022.112100

Teskey, R., Wertin, T., Bauweraerts, I., Ameye, M., McGuire, M. A., & Steppe, K. (2015). Responses of tree species to heat waves and extreme heat events. *Plant Cell and Environment*, *38*(9), 1699–1712. https://doi.org/10.1111/pce.12417

Tewari, M., Yang, J., Kusaka, H., Salamanca, F., Watson, C., & Treinish, L. (2019). Interaction of urban heat islands and heat waves under current and future climate conditions and their mitigation using green and cool roofs in New York City and Phoenix, Arizona. *Environmental Research Letters*, *14*(3), 034002. https://doi.org/10.1088/1748-9326/aaf431

Thom, J. K., Fletcher, T. D., Livesley, S. J., Grey, V., & Szota, C. (2022). Supporting growth and transpiration of newly planted street trees with passive irrigation systems. *Water Resources Research*, *58*, e2020WR029526. https://doi.org/10.1029/2020WR029526

UN-Habitat. (2020). *World cities report 2020: The value of sustainable urbanization.*

Walters, M., & Sinnett, D. (2021). Achieving tree canopy cover targets: A case study of Bristol, UK. *Urban Forestry and Urban Greening* 65, 127296. https://doi.org/10.1016/j.ufug.2021.127296

Wang, C., Wang, Z. H., & Ryu, Y. H. (2021). A single-layer urban canopy model with transmissive radiation exchange between trees and street canyons. *Building and Environment* 191, 107593. https://doi.org/10.1016/j.buildenv.2021.107593

Ward, K., Lauf, S., Kleinschmit, B., & Endlicher, W. (2016). Heat waves and urban heat islands in Europe: A review of relevant drivers. *Science of the Total Environment*, *569–570*, 527–539. https://doi.org/10.1016/j.scitotenv.2016.06.119

WWAP (2018). *The United Nations world water development report 2018: Nature-Based Solutions for Water*. Paris, UNESCO. ISBN 978-92-3-100264-9, www.unwater.org

Yang, Y., Endreny, T. A., & Nowak, D. J. (2013). A physically based analytical spatial air temperature and humidity model. *Journal of Geophysical Research Atmospheres*, *118*(18), 10449–10463. https://doi.org/10.1002/jgrd.50803

Yang, C., Yan, F., & Zhang, S. (2020). Comparison of land surface and air temperatures for quantifying summer and winter urban heat island in a snow climate city. *Journal of Environmental Management* 265, 110563. https://doi.org/10.1016/j.jenvman.2020.110563

Zhang, Y., Murray, A. T., & Turner, B. L. (2017). Optimizing green space locations to reduce daytime and nighttime urban heat island effects in Phoenix, Arizona. *Landscape and Urban Planning*, *165*(May), 162–171. https://doi.org/10.1016/j.landurbplan.2017.04.009

Ziter, C. D., Pedersen, E. J., Kucharik, C. J., & Turner, M. G. (2019). Scale-dependent interactions between tree canopy cover and impervious surfaces reduce daytime urban heat during summer. *Proceedings of the National Academy of Sciences of the United States of America*, *116*(15), 7575–7580. https://doi.org/10.1073/pnas.1817561116

Zölch, T., Maderspacher, J., Wamsler, C., & Pauleit, S. (2016). Using green infrastructure for urban climate-proofing: An evaluation of heat mitigation measures at the micro-scale. *Urban Forestry and Urban Greening*, *20*, 305–316. https://doi.org/10.1016/j.ufug.2016.09.011